*29th EPS Conference on Plasma Phys. and Contr. Fusion Montreux, 17-21 June 2002 ECA Vol. **26B**, P-2.078 (2002)*

Active Modification of the ELM Frequency in TCV

A W Degeling, Y R Martin, J B Lister, X Llobet

Centre de Recherches en Physique des Plasmas, Ecole Polytechnique Fédérale de Lausanne,

Association EURATOM-Confédération Suisse, 1015 Lausanne, Switzerland

Introduction. The detrimental effects of ELMs must be ameliorated or controlled if the ELMy H-mode is to be considered a viable scenario for future fusion reactor experiments such as ITER. Since the ELM amplitude is found to scale with the delay between ELMs, a possible approach to this goal could be to control the ELM frequency (f_{elm}), in order to avoid ELMs with large amplitudes. In order to explore how ELMs may be controlled, it is necessary to investigate what types of perturbations affect their dynamics. This paper reports: 1) Observations of intermittent phase locking between ELMs and Sawtooth dynamics on TCV, with entrainment of the ELM frequency to simple integer ratios of the sawtooth frequency (f_{st}); 2) A first attempt on TCV to actively modify the ELM frequency by applying a fast voltage perturbation to the radial field vertical control coils during single null ELMy H-mode discharges.

ELM - Sawtooth Synchronisation. ELM and Sawtooth cycles have periods that are of the same order of magnitude in TCV, which enables the possibility of their dynamics becoming coupled. Evidence of coupling comes in the form of frequency entrainment and phase locking between the two systems. These behaviours are clearly evident from f_{elm} and f_{st} time-series of individual discharges, however a more general result is shown by building a database using all the ELM occurrence times from a large number H-mode discharges (100 were used) and histogramming the ratio of f_{elm} to f_{st}, as shown in Fig. 1a). This figure clearly shows two peaks, centred at 1.0 and 1.7. The peak at 1.0 demonstrates that a large percentage of ELMs are strongly correlated with the sawtooth frequency.

An interesting result is found by plotting the histogram of the time delay between each sawtooth crash (using a centrally viewing soft X-ray chord) and the next ELM $\Delta t_{st\text{-}elm}$, as shown in Fig. 1b). This figure shows a sharp peak at $\Delta t_{st\text{-}elm} = 0$, followed by a minimum at 0.9 ms, and a broad maximum at 2 - 6 ms.There are at least two simple interpretations of this figure: 1) The peak at $\Delta t_{st\text{-}}$

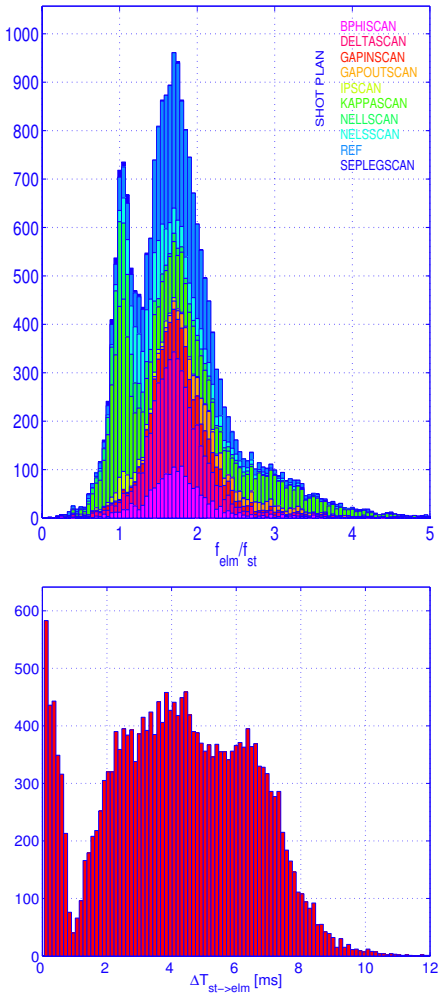

Figure 1: Histogram of f_{elm}/f_{st}, showing discharge categories in which a particular parameter was scanned; Histogram of $\Delta t_{st\text{-}elm}$

$_{elm}$ = 0 corresponds to ELMs immediately caused by the sawtooth crash (i.e. within 50μs). At these times, if the edge conditions are close to the stability threshold of ELMs, global MHD activity associated with the sawtooth may trigger an ELM; 2) The minimum occurring 0.9ms after the sawtooth crash corresponds to the measured arrival of the sawtooth heat pulse at the edge, which therefore has a stabilising effect on the ELMs, suggesting type III ELMs.

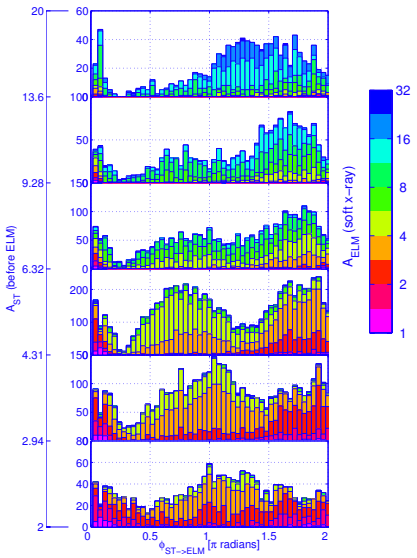

Figure 2: Histograms of the ELM phase in the sawtooth cycle with rows corresponding to increasing heat pulse amplitude [a.u.]

The phase of each ELM in the sawtooth cycle is defined in the database by $\phi = \Delta t_{st\text{-}elm} f_{st}$. Fig. 2 shows a series of histograms of the phase, in which the data has been segregated into rows on the y -axis using the amplitude of the last sawtooth heat pulse that arrived at the edge prior to each ELM (A_{st}, obtained from a soft X-ray chord with $\rho \sim 0.9$). Peaks in the histogram indicate a preferred phase that persists even in different discharges, and clearly indicates coupling. The appearance of a single peak as a function of ϕ corresponds to synchronisation with the fundamental f_{st}, while multiple peaks suggest a harmonic (or sub-harmonic, although this is rare). Fig. 2 shows that as the amplitude of the heat pulse increases, the peaks in the histogram become more apparent, indicating increasing coupling, and also that a transition from two peaks to a single peak occurs. Larger sawtooth crashes are correlated with high κ, and the single peak that forms with high A_{st} is mainly due to a series of discharges in which κ was scanned. This is also indicated in Fig. 1a) by the fact that the peak occurring at 1.0 is mostly comprised of counts from the 'kappascan' category. The histogram colours in Fig. 2 correspond to the size of the decrease in soft X-ray emissivity at the edge ($\rho \sim 0.9$) caused by each ELM, and show that larger amplitude ELMs occur as A_{st} increases. Parameter cuts were made in the database to investigate how the coupling varied with plasma parameters. Fig. 3a) and 3b) show the phase histograms for ELMs preceded by a sawtooth with $A_{st} > 4$ as a function of q_{95} (with $\kappa < 1.9$) and lower triangularity δ_L (with $q_{95} > 2.7$) respectively. The histograms in each case become more peaked as either q_{95} is increased, or δ_L is decreased, which indicates that coupling strengthens with δ_L and weakens with q_{95} .

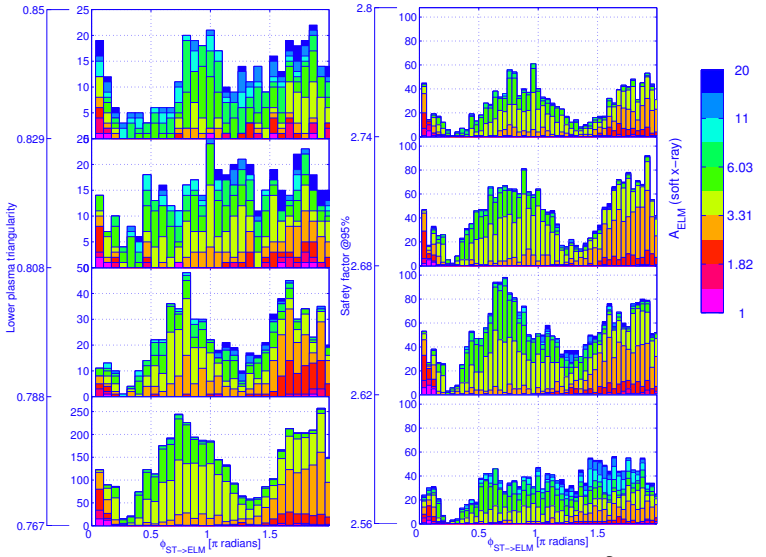

Figure 3: Histogram of ϕ with bins of increasing δ_L; Histogram of ϕ with rows of increasing q_{95}

Active ELM Control Experiments. The fact that the ELMs become synchronised with sawteeth suggests the possibility of actively controlling ELMs with an external driver signal. In this experiment, a fast voltage perturbation is applied to the radial magnetic field coils (G-coils) during single null ELMy H-mode discharges with stationary conditions. The G-coils are located at the top and bottom of TCV within the vacuum vessel and are routinely used for feedback vertical stabilisation. A perturbing signal was added to the vertical stabilisation feedback loop and consisted of a series of square pulses of 1ms duration, with a variable delay between pulses. This produced spike - like pulses in the current to the G-coil (up to 2kA) that resulted in deviations in the plasma vertical position of up to 5 mm. Figures 4 and 5 show two examples in which a constant amplitude pulse train was applied to the G-coil with an increasing driving frequency f_D from 143 to 330 Hz. The top graph in each figure shows a detail of the input signal, and the four following graphs show: the D_α timeseries (showing ELM times), the G-coil current, the timeseries of f_{elm} and f_D, and the phase of the ELMs with respect to the driving signal. The example in Fig. 4a (discharge 20332) shows that the perturbed current in the G-coils is roughly the same magnitude as the control system feedback signal produced by each ELM event, and that no phase synchronisation of frequency tracking occurs. Fig. 5 shows that when the G-coil current perturbation is increased to over 1 kA, the ELM frequency tracks the driving frequency, and the phase maintains a roughly constant value, interspersed with momentary losses in the phase locking. The vertical movement of the plasma caused by the perturbation is measured using magnetic pick-up coils, and gives some insight into how the perturbation might be affecting the ELM dynamics. Fig. 6 shows the results from a series of discharges in which frequency of the pulse train was swept as described above, while the amplitude and polarity of the pulse was varied from discharge to discharge. For each discharge, the range in driving frequency Δf overwhich the ELM phase was clearly affected by the perturbation was estimated and compared with the amplitude of the vertical displacement Δz associated with the perturbation. This figure shows that Δf clearly increases with Δz, that is, the frequency range overwhich ELM dynamics can be affected scales with the applied vertical displacement. We now turn to the question of how these vertical displacements affect the ELM frequency.

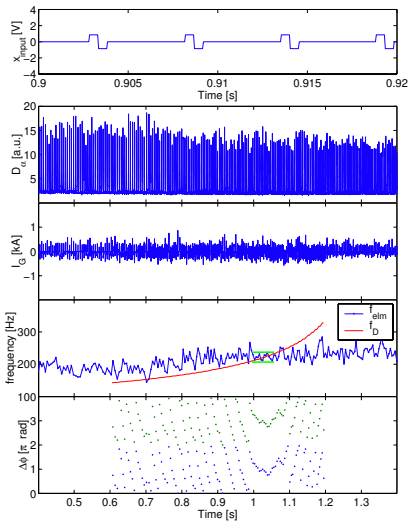

Figure 4: # 20332 Detail of the input signal; D_α time series; G-coil current; f_{elm} (blue), f_D (red) & Δf (green) overwhich f_{elm} is affected by f_D (negligible in this case); ELM phase w.r.t. driver

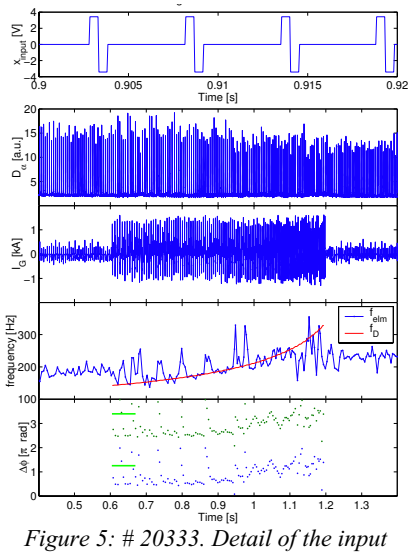

Figure 5: # 20333. Detail of the input signal; D_α time series; G-coil current; f_{elm}, f_D & Δf (green) overwhich f_{elm} is affected by f_D; ELM phase w.r.t. driver

It is generally considered that ELMs occur when a threshold for an MHD instability is exceeded, either in edge current

density (e.g. Peeling mode) or pressure gradient (e.g. Ballooning mode).We should therefore consider how the perturbation we apply affects these parameters. If we make the first order approximation that the plasma current displacement is then pressure gradients are not affected by plasma movement. The edge current density is given by $V_{surf} = 2\pi R\eta j_{\phi surf}$, where R and η are the major radius and resistivity, and the surface loop voltage is $V_{surf} = -\frac{d}{dt}\langle\psi_{ext}\rangle = -\langle\frac{\partial\psi_{ext}}{\partial t} + u\cdot\nabla\psi_{ext}\rangle$ and ψ_{ext} is the vacuum poloidal flux. Writing $V_{surf} = V_0(1+\varepsilon(t))$, then to 1st order for vertical displacements $u = \dot{z}$, $V_0 = -\langle\frac{\partial\psi_\Omega}{\partial t}\rangle \approx V_L$ and $\varepsilon = \langle\left(\frac{\partial\psi_G}{\partial t} + \frac{\partial\psi_{VG}}{\partial t} + u\frac{\partial\psi_\Omega}{\partial z}\right)/\frac{\partial\psi_\Omega}{\partial t}\rangle$, where ψ_W is the flux from the ohmic and shaping coils, ψ_G and ψ_{VG} are respectively the flux from the G-coil currents, and their vessel image currents, and <> indicates averaging over the last closed flux surface. The first two terms nearly exactly cancel at the location of the roughly centred plasma, hence $\varepsilon \approx \frac{u}{V_L}\langle\frac{\partial\psi_\Omega}{\partial z}\rangle$. Estimating u from the I_p*z measurement and numerically calculating the integral around the last closed flux surface gives ε ~ 0.1 for discharge 20333. That is, we estimate that the edge current density is being perturbed by about 10% by the externally driven vertical displacements. Such a perturbation might reasonably be expected to affect ELM dynamics.

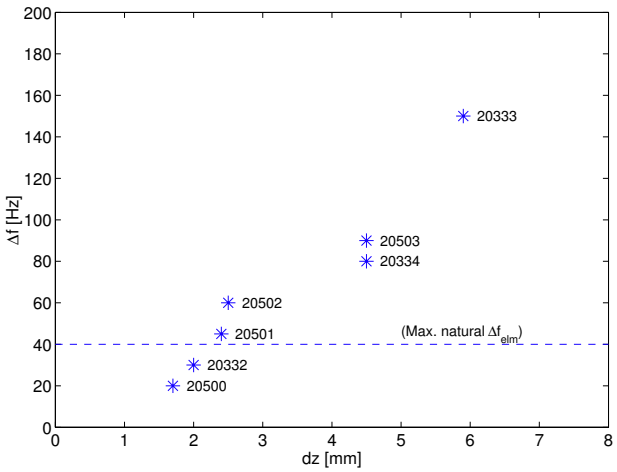

Figure 6: Driver frequency range overwhich ELMs appeared to be affected versus the amplitude of the vertical perturbation. The dashed line indicates the unperturbed f_{elm} fluctuation level. Points below this line indicate discharges in which the perturbation had no detectable effect.

Conclusions. Observations of the ELM and sawtooth time-series from TCV ohmic H-modes show that the two dynamical systems are frequently synchronised, with the ELM frequency related to the sawtooth frequency by an integer multiple. It was found that sawteeth affect ELMs in two different ways: 1) When the edge conditions are close to the ELM stability threshold, the occurrence of a sawtooth immediately triggers an ELM; 2) A more general coupling that results in a preferential phase for the ELMs in the sawtooth cycle and is dependent on the heat pulse amplitude, plasma shape parameters and q_{95}. A first attempt to actively control the ELM frequency was made by applying an external perturbation to the radial field vertical position control coils inside the vacuum chamber of TCV. It was found that the ELM dynamics became phase locked, and tracked the frequency of the applied signal when the amplitude of the perturbation was sufficiently large - albeit with intermittent breakages in phase lock. Coupling between the driver and the ELMs increased with the vertical displacement caused by the radial field, which strongly suggests that the ELM dynamics are being affected by perturbations in the edge current density.

The authors sincerely thank the TCV Team, without whom these experimental results would be unavailable. This work was partly supported by the Swiss National Science Foundation.